# Experimental study of the K-regime of breakdown in straight and swept wing boundary layers

V. G. Chernoray
*Institute of Theoretical and Applied Mechanics, 630090 Novosibirsk, Russia*

A. A. Bakchinov
*Chalmers University of Technology, Thermo and Fluid Dynamics, 41296 Göteborg, Sweden*

V. V. Kozlov
*Institute of Theoretical and Applied Mechanics, 630090 Novosibirsk, Russia*

L. Löfdahl
*Chalmers University of Technology, Thermo and Fluid Dynamics, 412 96 Göteborg, Sweden*

(Received 16 October 2000; accepted 28 February 2001)

In this Brief Communication, the nonlinear evolution of periodical disturbances generated by an external sound field in a swept wing boundary layer is presented. All experimental results are compared with corresponding data for a straight wing configuration. The Tollmien–Schlichting instability has been studied, and it was found that the disturbance flow field remained highly deterministic and periodic in both time and space until the latest stages of the transition. A frequency-wave number Fourier analysis shows that the disturbance spectra comprise only the fundamental wave and its higher harmonics. The K-type breakdown scenario was observed, and the nonsymmetry of flow patterns in the swept wing boundary layer was found to be due to the presence of the cross flow. © *2001 American Institute of Physics.* [DOI: 10.1063/1.1366667]

It is well known that the surface friction is the main source of drag on aircraft wings, road vehicles, and other streamlined bodies. Since the skin friction of turbulent boundary layers is significantly greater than that of laminar boundary flows, it is most important to have an insight into how the laminar–turbulent transition occurs in different three-dimensional (3D) boundary layers. This knowledge would enable prediction and, in a future perspective, also control of all stages of the transition.

Whereas the stability of two-dimensional (2D) boundary layers has been extensively studied theoretically, experimentally, and numerically, much less effort has been devoted to the stability of 3D boundary layer flows owing to complexity of phenomena underlying the breakdown of laminar to turbulent flow.[1] Experiments on swept wing flows have revealed that different transition mechanisms can dominate in a given flow. The main instabilities are viscous, so-called Tollmien–Schlichting (T-S) instability, Görtler instability, cross-flow instability, and attachment-line instability. Although the cross-flow instability is considered to be the most ''dangerous'' one, our current work is directed toward studies of the transition caused by the unstable T-S waves which can be observed in various 3D flows (e.g., boundary layers over straight and swept wings).

For 2D wall-bounded shear flows, two major types of transition are considered. At low levels of external perturbations the ''classic'' T-S transition scenario is observed, whereas the so-called ''bypass'' transition scenario is associated with a rather high level of environmental disturbances. The linear stability theory deals with the prediction of whether a given flow is stable or not, and the theory can predict the onset of transition and describe the initial linear stage. As far as the nonlinear wave evolution is concerned, two main regimes of transition have been identified and investigated experimentally, the K-regime, after Klebanoff *et al.*,[2] and the N-regime, experimentally studied for the first time by Novosibirsk group.[3] In the experimental work[4] it has been shown that both the initial spectral composition of interacting T-S waves and their initial amplitudes predesignate which of these regimes (competing with each other) occurs after the linear stage.

After the pioneering detailed experimental investigation of the K-breakdown scenario by Klebanoff *et al.*,[2] several experimental and theoretical studies have been conducted to adequately describe this phenomenon (e.g., see Refs. 5–8). The N-regime of transition was studied experimentally in detail a few years later (e.g., see Refs. 3,4,9–11). Comparisons between these two types of transition were discussed in Saric *et al.*,[4] Bake *et al.*,[10] and Laurien and Kleiser.[12] However, there is still a lack of experiments and computation covering the nonlinear evolution of disturbances in 3D boundary layer flows on airfoils at different sweep angles. In order to fill this gap, the generation and evolution of the viscous eigenwaves in 3D swept wing boundary layers have been experimentally studied and some of the results are presented in this Brief Communication.

The experiment was conducted in a closed-circuit wind tunnel with a test section of 1.8 m width, 1.2 m height, and 3 m length. A major series of experiments was conducted with the free-stream velocity $U_0$ equal to 12.8 m/s. The free-stream turbulence level in the test section was below 0.001 $U_0$ in the velocity range $U_0 = 5-15$ m/s (rms was calculated in a frequency range 0.1–10 000 Hz). All experiments were performed with a C-16 wing profile (500 mm chord, 1500

 

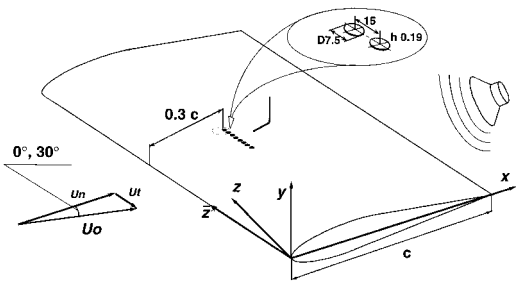


FIG. 1. Schematic of the experimental setup and the coordinate system.

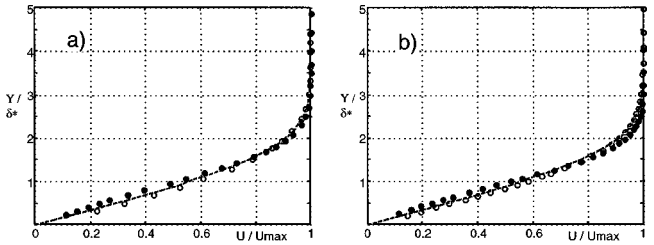


FIG. 3. Mean streamwise velocity profiles on straight (a) and swept (b) wings compared with Blasius profile. $X/c=0.32$—open circles, $X/c=0.48$—filled circles.

mm long, and 80 mm thick, Fig. 1). The airfoil was mounted horizontally in the middle of the wind-tunnel test section, but the main series of experiments was performed at two sweep angles, namely at zero (a straight wing configuration) and 30 deg (a swept wing configuration). The attack angle of the wing was chosen to give a weak adverse streamwise pressure gradient distribution in the measurement region over the working side of the airfoil: see Fig. 2. In this and subsequent figures the streamwise coordinate $X$ is scaled with the wing cord, $c$, which is equal to 500 mm for the straight wing configuration and 580 mm for the swept wing configuration. At this angle of attack no local separation of the flow was observed on the airfoil.

It was found that the transition to turbulence for both configurations was provoked by a rather high level sound field at a frequency $F_0=300$ Hz. To obtain spatial-temporal flow patterns of the disturbed boundary layer, the data acquisition was triggered with a signal from a microphone located in the test section.

To control a spanwise variation of the disturbance flow field, roughness elements were placed on the surface and equidistantly aligned along the airfoil leading edge. The roughness elements stabilized the peak-and-valley $Z$-distribution of the wave amplitude and allowed studies of 3D patterns of the transitional boundary layer flow at both linear and nonlinear stages. The roughness array consisted of ten cylindrical humps (7.5 mm diameter and 0.19 mm height) with a spacing of $\Delta Z_0=15$ mm (see Fig. 1 for details), and as positioned at the chord region $X/c=0.30$ where the streamwise pressure gradient changed its sign from negative to positive. Previous experiments have clearly shown that in this region acoustic disturbances transform into eigenoscillations of the boundary layer (i.e., the highest receptivity of the boundary layer to acoustic waves was observed). The local Reynolds number based on the displacement thickness $\mathrm{Re}_{\delta^*}$ at the position of humps was about 600 and 640 for straight and swept wing configuration, respectively, which corresponded to the boundary layer thickness $\delta$ of 1.78 and 1.87 mm. Detailed mapping of the flow was made by a single, constant temperature hot wire, and the spanwise velocity component (cross flow) was measured with a conventional $V$-shaped two-wire boundary layer probe. The distance between centers of the wires was 1.2 mm, and the signals were then ensemble averaged over 300 realizations and stored in a PC for subsequent analysis.

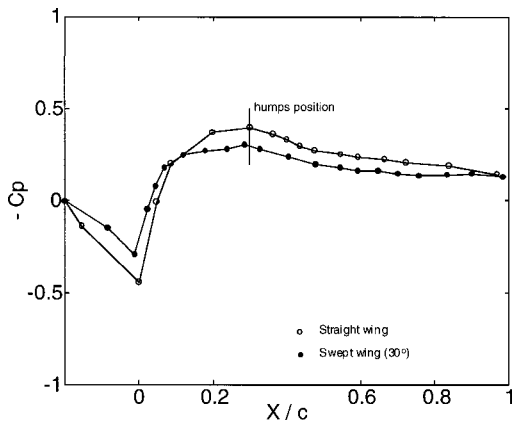


FIG. 2. Chordwise pressure coefficient distribution for straight and swept wing configurations.

As can be seen from Fig. 2 the weak adverse pressure gradient was established on the wing surface from $X/c=0.3$ for both configurations. Magnitude of the pressure gradient parameter $dCp/d(X/c)$ was less than 0.9 in both cases. In the range of $X/c=0.5$–$0.7$ the pressure grows monotonically at about equal rates. The distribution of $Cp$ does not reveal any local separation behavior of the flow (there is no constant pressure plateau). Figure 3 shows profiles of mean streamwise velocity measured at $X/c=0.32$ and 0.48 (the corresponding Blasius profiles are shown with dotted lines). At the first streamwise position the profiles are full, but further downstream they reveal a decrease of the velocity near the wall for both straight and swept wing configuration.

Transformation of the sound, at 300 Hz frequency, into boundary layer waves was observed at $X/c=0.3$ for both sweep angles. Waves grew as $X$ increased, and resulted in the fully turbulent boundary layer flow at the last positions measured, $X/c=0.9$. Amplitude-frequency spectra of some characteristic time traces are shown in Fig. 4. The nonlinear evolution of the waves undergoes the stage of generation of super harmonics (600, 900 Hz, etc.). Further downstream resonant and combinational interactions between the waves and random background disturbances eventually lead to complete randomization of the flow and typical turbulent spectra shown at $X/c=0.9$. The first observation to be made is that the nonlinear evolution looks identical for both straight and swept wing configurations, and the second is that the transition on the straight airfoil seems to occur somewhat earlier than that on the swept wing due to different flow parameters (Reynolds number, pressure distribution). The time traces have been measured in the boundary layer at a

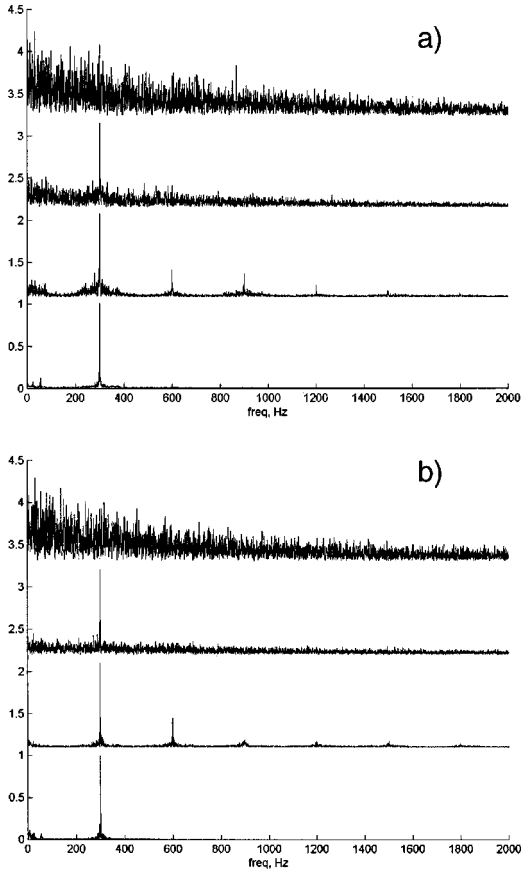


FIG. 4. Amplitude-frequency spectra of time traces measured in straight (a) and swept (b) wing flows for different positions from leading edge at $X/c$ $=0.6$, 0.7, 0.8, 0.9 (from bottom to top), $Y=$const. Each spectrum is normalized with its maximum value.

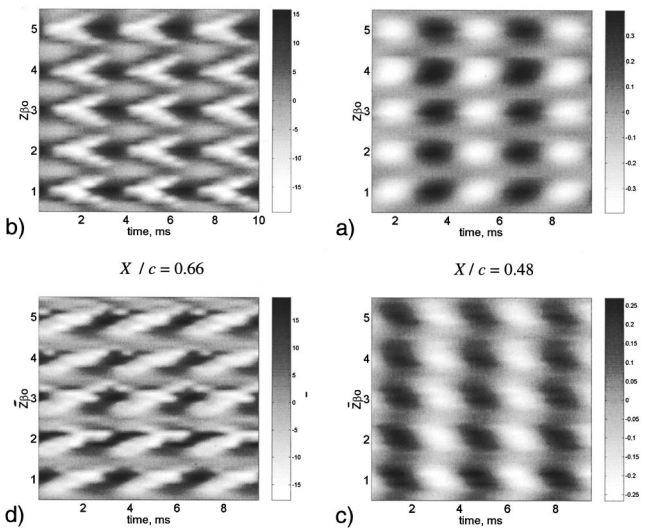


FIG. 5. Patterns of the ensemble-averaged streamwise velocity disturbance component in $(t,z)$ planes demonstrating two scenarios of transition in straight (a, b) and swept (c, d) wing flows. $X/c=0.48$ (a, c), $X/c=0.66$ (b, d). The flow direction is from right to left.

constant distance $Y$ from the airfoil surface at $Z=0$ (the center of a roughness element).

Measurements in the spanwise direction revealed that the modulated waves in that direction were observed for both configurations. Maxima in the spanwise wave amplitude distributions were found at the position of the spacers ($Z\beta_0$ $=1,2,\ldots,$ where $\beta_0=1/\Delta Z_0$). At the downstream position $X/c=0.48$, the amplitude of the waves was measured and equal to 0.39% $U_\infty$ and 0.27% $U_\infty$ for the straight and the swept wing, respectively, where $U_\infty$ a local streamwise velocity of the inviscid flow. The phase velocity of the waves $c_r$ was found to be $0.41U_0$ ($\alpha_r=17.5$ mm) with the wavefront parallel to the leading edge. In the case of the straight wing configuration the spanwise modulation of the wave is symmetrical and corresponds to a combination of the plane spectral mode $(F_0,0)$ and two oblique modes $(F_0,\pm\beta_0)$ in Fourier space (not shown). For the swept wing the modulation does not seem to be symmetrical and the corresponding frequency-spanwise wave number spectra consist of the mode $(F_0,0)$ and only one oblique mode $(F_0,\beta_0)$. Nonlinear interacting waves grow downstream with formation of ''peak'' and ''valley'' structures in the spanwise directions. High amplitudes of perturbations were found in peak positions. On Fig. 5, left, at $X/c=0.66$ the nonlinear stage of disturbance development is shown. The amplitude of disturbances is more than 15% of $U_\infty$ for both configurations.

In the straight wing boundary layer so-called $\Lambda$ structures similar to those observed by Klebanoff *et al.*[2] were mapped, whereas in the swept wing boundary layer nonsymmetrical structures were obtained.

It should be noted that nonsymmetry of the basic (mean) boundary layer flow (for the swept wing) results in nonsymmetry of the disturbance flow patterns at the nonlinear stage of evolution of the waves (see Fig. 5). Fourier decompositions (not shown) reveal the growth of modes $(F_0,\pm 2\beta_0)$ in the case of straight wing (formation of ''legs'' of the $\Lambda$ structures). Evolution of the spectra for the swept wing configuration differs from that for the straight wing. At the initial stages of the nonlinear evolution damping of the $(F_0,\beta_0)$ mode takes place accompanied by the amplification of the antisymmetrical $(F_0,-\beta_0)$ mode. Further downstream, the growth of the $(F_0,-2\beta_0)$ mode occurs accompanied by the decaying $(F_0,0)$ mode. Flow structures shown in Fig. 5(d) are mostly associated with modes $(F_0,0),(F_0,-\beta_0)$, and $(F_0,-2\beta_0)$. As we pointed out above, the main reason for the nonsymmetry for the flow patterns is the presence of the cross flow.

Experiments by Grek *et al.*[13] showed that the cross flow could cause the formation of nonsymmetry in streaky structures. In their experiments, a solitary streaky structure was generated in the boundary layer by means of injection of a portion of air through a transversal slot on the swept wing surface. To check those results, detailed measurements of cross flow have been done (Fig. 6). In the boundary layer of the swept wing our measurements have shown that the nonzero cross-flow velocity component, $W$, can be observed in all streamwise positions measured. At the position of roughness elements, $X/c=0.3$, the magnitude of the $W$ velocity was found to be up to 10% of $U_0$ inside the boundary layer, and about 6% of $U_0$ at the outer edge of the boundary layer. Further downstream the cross-flow component is almost constant from $X/c=0.5$ to $X/c=0.8$ with magnitude of 3% of $U_0$.

The step on the inner curve at $X/c=0.3$ (see Fig. 6) is

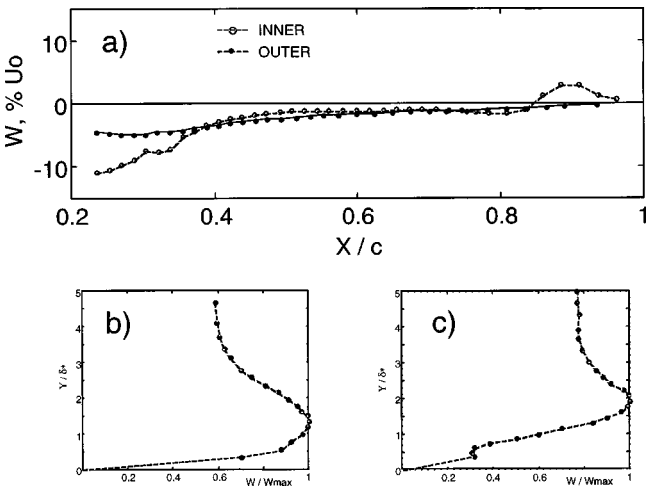


FIG. 6. Results of cross-flow measurements on the swept wing. Chordwise mean cross-flow distribution (a) for inviscid flow (outer) and flow inside boundary layer (inner). Distribution of mean cross-flow velocity across boundary layer: $X/c=0.32$, (b) and $X/c=0.48$ (c).

due to streamline displacement caused by the roughness elements. After $X/c=0.85$ the cross-flow component of velocity changes its sign from negative to positive. Figure 5 shows $\Lambda$ structures in $(Y, Z, t)$ coordinates for straight wing and nonsymmetrical structures for the swept wing flow. It is evident that structures in both cases are different not only at one given $Y$ position, but across the boundary layer. A high-shear layer is formed near the ''head'' and ''shoulders'' of the lambda structures in the straight wing flow, as it was observed in experiments on the flat plate boundary layer.[2,3,6,10] In a swept wing flow there are two regions of high-shear layer along each structure. It can be concluded that, due to the cross flow, the temporal-spatial structures of the disturbed flow field over the swept wing have revealed significant differences in K-type transition to turbulence.

Experiments on the stability of three-dimensional boundary layers on straight and swept airfoils have been conducted. Detailed measurements of the streamwise velocity field in $(Y, Z)$ planes, as well as 3D frequency-wave number spectra have revealed linear and nonlinear evolutions of the disturbances generated by an external acoustic field in the airfoil boundary layers. The Tollmien–Schlichting waves, excited by the sound, were dominant in both configurations, and the disturbance flow field was found to remain highly deterministic and periodic both in time and space until the latest stages of the transition. The K-type transition was identified with the aligned order of so-called lambda patterns at the nonlinear stage of the transition. The nonsymmetry of flow patterns in the boundary layer flow was caused by the cross flow in the swept wing case (see Fig. 7). To the best of our knowledge this is the first experimental work where the K-regime of transition on a swept wing model has been observed and compared with that on the straight wing model with other conditions been equal.

## ACKNOWLEDGMENTS

This work was supported by the Royal Swedish Academy of Sciences, and the visit of V.V.K. and V.G.C. to Chalmers University of Technology was made possible through this exchange program.

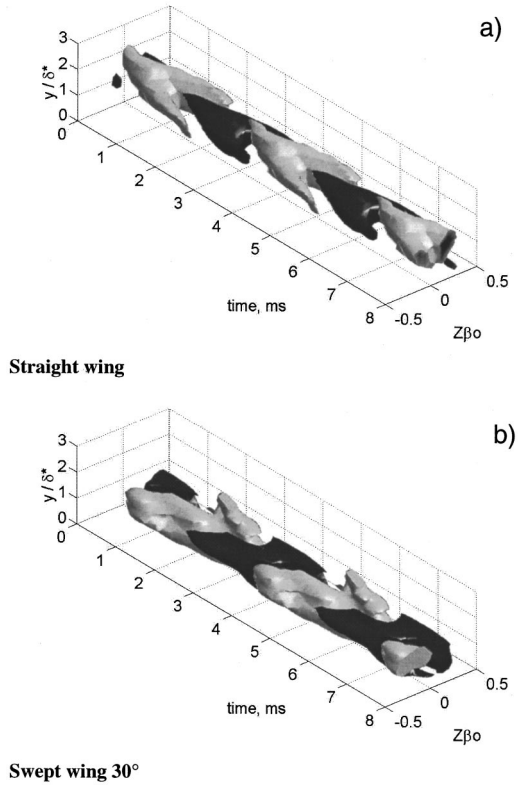


FIG. 7. Isosurfaces of the ensemble averaged streamwise velocity disturbance component $u=0.08U_\infty$—dark shading, $u=-0.08U_\infty$—light shading. $X/c=0.66$. $\Lambda$ structures in straight wing flow (a); nonsymmetrical structures in the swept wing boundary layer (b).

[1]H. L. Reed and W. S. Saric, ''Stability of three-dimensional boundary layers,'' Annu. Rev. Fluid Mech. **21**, 235 (1989).
[2]P. S. Klebanoff, K. D. Tidstrom, and L. M. Sargent, ''The three-dimensional nature of boundary layer instability,'' J. Fluid Mech. **12**, 1 (1962).
[3]Y. S. Kachanov, V. V. Kozlov, and V. Y. Levchenko, ''Nonlinear development of a wave in a boundary layer,'' Izv. Akad. Nauk SSSR, Mekh. Zhidk. Gaza **5**, 85 (1977) (in Russian) [Trans. Fluid. Dyn. **12**, 383 (1977)].
[4]W. S. Saric, V. V. Kozlov, and V. Y. Levchenko, ''Forced and unforced subharmonic resonance in boundary layer transition,'' AIAA Paper No. 84-0007 (1984).
[5]F. Harna and J. Nutant, ''Detailed flow-field observations in the transition process in a thick boundary layer,'' *Proceedings Heat Transfer and Fluid Mechanics Institute* (Stanford University Press, Stanford, 1963).
[6]Y. S. Kachanov, V. V. Kozlov, V. Y. Levchenko, and M. P. Ramazanov, ''Experimental study of the K-regime breakdown of a laminar boundary layer,'' Preprint 9-84, Inst. Theoret. Appl. Mech., USSR Acad. Sci., Novosibirsk (1984) (in Russian).
[7]T. Herbert, ''Secondary instability of boundary layers,'' Annu. Rev. Fluid Mech. **20**, 487 (1988).
[8]U. Rist and H. Fasel, ''Direct numerical simulation of controlled transition in a flat-plate boundary layer,'' J. Fluid Mech. **298**, 211 (1995).
[9]V. V. Kozlov, V. Y. Levchenko, and W. S. Saric, ''Formation of three-dimensional structures in a boundary layer at transition,'' Preprint No. 10-83, Inst. Theoret. Appl. Mech., USSR Acad. Sci., Novosibirsk (1983) (in Russian).
[10]S. Bake, H. H. Fernholz, and Y. S. Kachanov, ''Resemblance of K- and N-regimes of boundary layer transition at late stages,'' Eur. J. Mech. B/Fluids **19**, 1 (2000).
[11]H. Fasel, ''Numerical simulation of instability and transition in boundary layer flows,'' in *Laminar Turbulent Transition*, edited by D. Arnal and R. Michel (Springer, Heidelberg, 1990), p. 587.
[12]E. Laurien and L. Kleiser, ''Numerical simulation of boundary layer transition and transition control,'' J. Fluid Mech. **199**, 403 (1989).
[13]G. R. Grek, M. M. Katasonov, V. V. Kozlov, and V. G. Chernoray, ''Modelling of streaky-structures in two- and three-dimensional boundary layers,'' Preprint No. 2-99. Inst. Theoret. Appl. Mech., Russian Acad. Sci., Novosibirsk (1999) (in Russian).